Prabha Materials Science Letters
Vol. 4, No. 1, 107-118, 2025
https://doi.org/10.33889/PMSL.2025.4.1.010

Ram Arti Publishers

Molecular Modelling and Investigation of Bioactive Stable DNA G-Quadruplex d($G_4T_4G_4$) under Different Physiological Conditions using Molecular Dynamics Simulation

Jwala Ji Prajapati
Department of Physics,
Deen Dayal Upadhyaya Gorakhpur University, Gorakhpur, 273009, Uttar Pradesh, India.
E-mail: jwalajisjlt@gmail.com

Ramesh Kumar Yadav
Department of Physics,
Baba Raghav Das Post Graduate College, Deoria, 274001, Uttar Pradesh, India.
E-mail: rkybrd@yahoo.in

Umesh Yadava
Department of Physics,
Deen Dayal Upadhyaya Gorakhpur University, Gorakhpur, 273009, Uttar Pradesh, India
Corresponding author: u_yadava@yahoo.com

(Received on October 3, 2024; Revised on December 3, 2024; Accepted on December 9, 2024)

Abstract
We are reporting a molecular dynamics study on the structure and conformation of the DNA quadruplex. The single molecule quadruplex's coordinates were obtained and modeled using PDB ID 1d59. The simulation's sequence is d(GGGGTTTTGGGG). In the beginning, two hairpin structures were constructed with loops holding thymine residues at either end, forming a four-stranded helical structure. The cyclic hydrogen bonds created by the structure kept the guanine residues of all four strands in one plane. The molecule was subjected to molecular dynamics simulation for 100ns and at periodic intervals of 10ns, the dynamical pathway's trajectory was examined. The deviations and fluctuations viz. RMSD, RMSF and Rg plots were analyzed, the structure and shape of the time-evolved trajectory were examined. The outcome was compared with the crystal structure. Our findings reveal a few peculiar properties which we have discussed in this paper. The helix axis and torsion angle parameters were calculated. The results of this interpretation give the idea about quadruplex interaction with external agents and inspire to do further research on DNA quadruplex structures in telomeric regions of living chromosomes.

Keywords- G-quadruplex, G-tetrad, MD simulation, Oxytricha telomers.

1. Introduction

A non-canonical secondary structure (Non-Watson-Crick) of higher order DNA folded into a four-stranded structure rich in guanine, was found to form at the end of telomers in most telomeric sequences in chromosomes of cell. Four guanine(G) nucleic acid bases are connected together via a Hoogsteen type cyclic hydrogen bonding that kept the guanine residues of strands in one square plane, named as G-tetrad (**Figure 1**). These tetrads stack on top of each other in parallel and are further stabilized by a monovalent physiological cation (M^+ = K^+, Na^+, Li^+, etc) in cavity that is centrally coordinated to form G-quadruplexes. A quadruplex with no metal ion will become unstable (Largy et al., 2016; Spiegel et al., 2020). The telomeric sequences that constitute the G-quadruplex have a diverse character because of the interactions between molecular strands, so it can take distinct topologies and directions. In eukaryotic genomes as well as those of other organisms like bacteria and viruses, it is found to play a significant role in transcriptional and translational regulation of genes (Burge et al., 2006). Numerous studies on the G-4

quadruplex in various species have demonstrated that it controls the unusual growth of cells and tissues which results in mortality from diseases including cancer, Mtb, HIV and other pathogenic conditions. It has been suggested that DNA G-quadruplex (G4s) structures cause genomic instability and aid in the development of cancer. Considering G4s in cancer research is crucial, and it emphasizes the necessity of more research into the molecular pathways underpinning G4-mediated genomic instability (Neupane et al., 2023; Richel et al., 2024; Zhang et al., 2023). Here, we offer data and information collected close to physiological situations in order to improve the in-silico evolution of methods for future research and to anticipate the structure. Once the G-quadruplex pattern is disrupted, gene mutation can be avoided, and ligands or medications that can reassemble the gene to render it inactive and accountable for a biological or pharmacological interaction can be studied (Di Leva et al., 2014). G-quadruplexes have been studied theoretically using classical molecular dynamics (MD) simulation as well as quantum-mechanical modelling. The kinetics and structural analysis of different stranded quadruplex data have been studied computationally (Batool et al., 2019; Farag et al., 2023; Huppert and Balasubramanian, 2007; Largy et al., 2016). Furthermore, the comparison of ion interaction with nucleic acid bases has been performed using force-field methods. Through MD simulations, the dynamic behaviour of quadruplex formation has also been developed. MD simulation is a theoretical methods and computational techniques used to mimic and study the dynamic behaviour of molecules (Šponer et al., 2020).

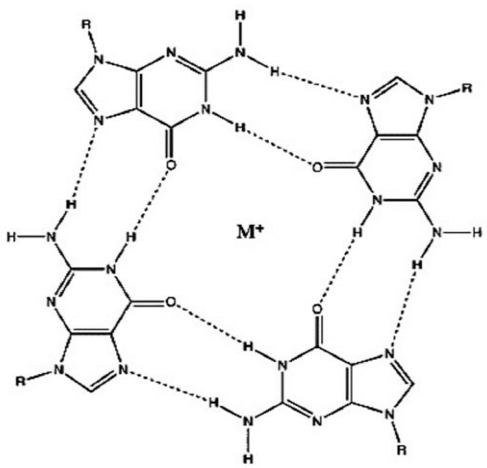

Figure 1. DNA Quadruplex structure showing hydrogen bonds in square planar ring.
(Haider et al., 2002, open access).

In order to understand the variability of the G-quadruplex, our work constructs new structural parameters and a biophysical conformation of the crystal structure of sequence d(GGGGTTTTGGGG) of Oxytricha telomer, a ciliated protozoan from the protein data bank of code 1d59 (Haider et al., 2002; Kang et al., 1992). For predictive research, the sequence was modelled and run via MD simulations. Numerous regulatory steps are involved in the study of DNA G-quadruplexes, which anticipate a great deal of information and provide as a foundation for additional research on the compound's chemical and drug-like behaviour and activity so that it can interact with some ligands that binds it with high affinity and reduce its efficiency (Bryan et al., 2020; Frasson et al., 2022; Ma et al., 2020). An increasing number of studies indicate that different nucleic/amino acids and ligands were involved in the regulation of biological processes, rather than G-quadruplexes acting alone. These days Numerous computational and experimental methods are available that have used to confirm the capability and activity of G-quadruplex. X-ray crystallography, NMR, and circular dichroism spectroscopy are a few techniques that offer

structural information about G-quadruplex and ligand interactions (Salgado et al., 2015). These techniques are also utilized to explain the dynamics of quadruplex production and to gather data on the thermal stability of quadruplexes. Regular expression matching techniques were first employed in the algorithmic development of quadruplex detection. The biophysical conditions against the stability of quadruplex, which is restricted by several biophysical techniques, have been validated by numerous computational methodologies.

The last few years have seen a great deal of significant research, the introduction of tiny medications that target G4 ligands from particular genes, and advancements in technology. The ability of binding and development medications has been made possible by the development of software and the investigation of the complex interactions taking place within the binding and active sites of DNA quadruplexes (Sun et al., 2019). Structural analysis can be used to investigate the conformational changes occur into G4 structure. There has been extensive use of the G-quadruplex in aptamer-based sensing systems. Adenosine, sugar, peptides, food toxins, protein (amino acids), and other tiny compounds can be detected using the G-quadruplex structure, which has been shown in some recent research to function as an adapter in the creation of fluorescence sensors. For the measurement of multiplexed mycotoxins, a G-quadruplex aptamer-encapsulated photonic crystal (PhC) barcode is utilized. Drug-targeted cancer treatment is another application for G-quadruplex. The human immune system disease AIDS is brought on by infection with the Human Immunodeficiency Virus (HIV), a member of the retrovirus family. To date, there is no particular drug or treatment that can cure this disease. In light of these, our goal was to select a distinct molecule of telomeric DNA whose crystal structure data was accessible so that we could contrast it with the data from our simulated structure (Ciaco et al., 2024; Farag and Mouawad, 2024; Nao et al., 2020; Zhang et al., 2023)

2. Methodology

2.1 Explicit Molecular Dynamics Simulation

The PDB entry 1d59 contains the coordinates of the DNA G-quadruplex of the sequence d(GGGGTTTTGGGG). Using a 10 Å × 10 Å × 10 Å simulation grid box, the DNA G-quadruplex was first protonated at neutral pH (7.0 ± 2) and then put in a Monte-Carlo equilibrated explicit transferable intermolecular potential (TIP3P) solvent as has been reported earlier. The Desmond package's system construction module was then used to neutralize the system's overall charge with an appropriate number of counterions. The chemical system in the simulation box is made up of 782 atoms in total, comprising quadruplex atoms and ions. In the beginning, two hairpin structures were constructed with loops holding guanine residues at either end, forming a four-stranded helical structure. In order to reach a slope threshold of 25 kcal/mol-Å, the system's energy was first minimized using the steps of the steepest decent method. Following equilibration, the system was subjected to the production of an MD trajectory as a function of 100 ns under the NPT ensemble coupled with the Desmond suite's OPLS (Optimized Potentials for Liquid Simulations) all atom force field. Here, the Ewald technique was used to evaluate long-range Coulombic forces. Additionally, the mathematical incorporation made use of Verlet leapfrog algorithm, with a time step duration of 1.0 fs for minimization and 2.0 fs for dynamics. For additional research, the best simulated structure found at the corresponding time increments of 10 ns was taken into consideration (Kang et al., 1992).

2.2 Analysis of Conformational Parameters

The DNA quadruplex is a dynamic molecule that is analysed by using X3DNA software. We have utilized the program X3DNA to determine the helicoidal and backbone characteristics and for the examination, reconstruction, and viewing of three-dimensional nucleic acid structure. In our investigation, ten snapshots from 100 ns dynamics were taken at intervals of 10 ns. In order to characterize the structural

deformability of DNA, the following parameters were examined: rises, groove widths, axis bend angles, slides, roll angles, and twist angles. Utilizing a rigorous matrix-based scheme to calculate local conformational parameters and reconstruct the structure from them, the program uses a reference frame to describe the geometry of nucleic acid base pairs. For the purpose of understanding the folding and rotation of bases during dynamical path way, helical parameters and torsion angle parameters are essential.

3. Results and Discussions

3.1 Structure of the DNA G-quadruplex in Various Modes

The examinations performed on quadruplex announced that it can adopt various topologies on the basis of nucleotide arrangements (Burge et al., 2006). Investigations of G-quadruplex can be done by computational simulation programs. At first, full-atomistic MD simulations were conducted for the selected DNA quadruplex to access the thermodynamics stability in solution and conformational properties of the simulated models were compared to that of crystal structure. The snapshots taken at periodic intervals of 10.0 ns MD simulation at 300K reveals systematic consistency in DNA quadruplex especially at the planar region of the model during the 100 ns MD simulation interval. Analysis of the extracted snapshot demonstrates the flexibility in the base pairs located mostly at the sides of square planar quartet. Slight folding of the strands is observed due to the conformation change in the guanine base pair plane with respect to adjacent bases getting closure to each other. At this temperature, none of the snapshots exhibit abrupt disturbance that indicate the stability and integrity of G4 structure.

3.2 Analysis of Torsion Angles Parameters

In addition, the DNA quadruplex model's individual backbone torsion angles (α, β, γ, δ, ε, z, η, and χ) for each nucleotide were calculated. For the initial structure, or pre-dynamics (**Table 1** & **2** for initial structure), the torsion angles computed for the MD simulation, which was performed at 300K temperature for 100 ns, (**Table 3** & **4** for final structure). The wide conformational space is denoted by the terms ±Gauche (±g) and trans (t), while Klyne-pre-log notation, such as Syn, Anti, Synclinal (sc), and Anticlinal (±ac), is employed for further in-depth study. Based on these Tables, we can see that there is a significant correlation in the conformational activity between torsion angles α. For both the first and second strand, the majority of residues have torsion angles that oscillate within gauche(g-) and gauche(g+) areas, respectively. For most of the first and second strand residues, there is a significant dynamical excursion in the trans regions of the torsion angle γ. The first and second strand's anticlinal (ac) regions are displayed by the torsion angles δ. For both strands, the torsion angles ε and z freely oscillate in the gauche(g-) and -synclinal (-sc) regions. Comparable patterns can be seen in the glycosyl angle (χ), which primarily hovers in the ac to ap regions for most residues in the first and second strands of the molecule (except for G5, G10, and G15, which are in the g+, t+, and g+ regions, respectively). Despite the fact that the sugar rings for the first and second strands exhibit significant dynamical excursion into the C2'-exo to C2'-endo regions Following dynamics, the majority of sugar rings oscillate between the C1' -Exo and C1' -Exo regions. When we compare the standard values of corresponding conformational parameters of various DNA types with the various conformational parameters obtained by the X3DNA program of the original structure, we find that, despite some differences, the various parameters of the original structure and the MD simulated structure are close to the expected ranges for B type DNA (Watson-Crick base model).

Table 1. Torsion angle parameters: strand- I for the initial structure of DNA G-quadruplex.

S. No.	base	alpha	beta	gamma	delta	epsilon	zeta	chi
1.	T	144.3	163	168.8	83.9	-163.3	-30.1	-168.9
2.	G	87.3	136.7	-146.7	90.9	…...	….	-164.5
3.	G	…….	…...	-93.1	134.1	178.1	-95.4	44.5
4.	G	112.2	-132.8	-164.4	84	-136.9	-48	-7.5
5.	G	-174.1	145.9	165.7	150.6	-129	-15.7	-165.2
6.	G	-119	61.4	-171.2	100.7	153.6	38.7	-8
7.	G	-115	-134.6	90.7	76.4	82.5	81.9	168.6
8.	G	-174.7	85.8	143.9	89.9	158.9	-18.9	-173.4
9.	T	153.9	155.1	177.5	154.2	-149.9	-71.8	-106.5
10.	G	…...	…...	-115.1	131.7	81.2	-62.5	134.4
11.	T	138.3	146.9	-153.2	75.5	-174.5	-48.7	-159.9
12.	G	102.2	150	-97.6	155.4	…..	…….	-113.4
13.	G	169.9	164.4	173.3	76.5	-159.3	-43	-13.8
14.	G	-69.6	-71.2	-152.6	111	-143.4	-82	29.4
15	G	163.6	172.8	87	94.1	124.6	-79.6	-31.2
16.	G	-58.4	-56.1	-158.1	84.9	-179.3	1.4	2.2
17.	G	-41	160.1	62.3	119	41.6	84.7	64.6
18.	G	145.7	147.6	177.1	91.8	…...	….	175.6
19.	T	78.6	139.8	-169	140.1	152.4	-110.4	131.7
20.	G	…….	….....	-129.9	108.4	176.6	-121.2	17.6

Table 2. Torsion angle parameters: strand II for the initial structure of DNA G-quadruplex.

S. No.	base	alpha	beta	gamma	delta	epsilon	zeta	chi
1.	T	161	-120	122.7	70.4	176.5	-84.7	-115.6
2.	G	-79.7	90.3	162.3	79.5	-152.4	-30.3	-27.2
3.	G	98.4	146.6	145.1	155.9	-178.4	-115	-122.7
4.	G	-86.7	176.3	41.3	146	-64.8	-133	-117.5
5.	G	-164.9	120.3	146.1	81.5	145.6	49.7	-37.2
6.	G	97.4	136.2	-172.9	146.3	-165.2	-132	-132.1
7.	G	-53.2	-60.1	-157.8	82.4	-159.6	6.2	6.1
8.	G	58.7	178.2	173.2	124.7	44	62.3	91.3
9.	T	127.2	128.7	-158.1	99.8	25.2	83.3	74.5
10.	G	177.8	111.1	177.5	148.2	….	…...	-172.6
11.	T	33	-158.8	-70.1	85	-126.1	173.8	55.7
12.	G	90.9	-127.2	-170.9	126	-167.1	-112.3	40
13.	G	18.3	138.7	-19	161.4	-82	-126.4	-97.6
14.	G	169.2	-124	158.4	88.2	-116.3	-35.2	-169.9
15.	G	109.8	76	173.8	72.9	173.2	65.5	-27.2
16.	G	140	114.4	167.5	141.5	147.1	92.9	-173.3
17.	G	-172.2	91.6	123.9	86.3	79	58.3	-173.8
18.	G	…….	…….	-144.4	121.3	72.6	67.4	84.6
19.	T	59.3	-172.7	-143.9	149.2	-141.3	-60.6	-98.2
20.	G	-134	122.9	101.3	84.4	175.7	-34.7	-166.2

Table 3. Torsion angle parameters (strand I) for the final structure(100ns).

S. No.	base	alpha	beta	gamma	delta	epsilon	zeta	chi
1.	G	-95.8	56.4	161.8	109.5	-81.5	-58.7	53.4
2.	G	-82.1	61.9	173.3	113.2	-101.6	-57.6	-128.3
3.	G	-87.1	44	164.6	86.4	11.2	-59.6	-145.6
4.	G	-82.4	53.3	172.7	123.3	-----	-----	-87.9
5.	G	-----	-----	-178.1	115.3	-61.3	70.8	-131.1
6.	T	-80.4	51.4	167.2	135.1	-87.2	-159	-159.2

Table 4. Torsion angle parameters (strand II) for the final structure(100ns).

S. No.	base	alpha	beta	gamma	delta	epsilon	zeta	chi
1.	G	-77.3	79.4	172.9	100.6	-96.9	-68.4	-136.4
2.	G	-74.3	30.2	178.3	109.3	-86.2	-70.8	78.5
3.	G	-76.5	32.7	177.6	142.7	-88.6	-74.4	-117.8
4.	G	-81.3	54.9	177.8	105.6	-106.2	-67.2	-128.1
5.	G	-81.8	64	158.8	108.2	-86.8	-53.5	40.1
6.	T	-82.2	34.8	171.2	85.1	-100.7	-84.9	43.3

3.3 Examination of Helicoidal Parameters

The starting structure's helicoidal characteristics as well as the structures derived from a 100 ns molecular dynamics simulation are tabulated. The X3DNA program has been used to calculate each and every helicoidal parameter. Subset of helicoidal parameters that include X-disp, Y-disp, h-Rise are distance parameters while inclination, Tip, h-twist are angle parameters (**Table 5**, **Table 6**). Shear, Stretch, and Stagger are distance parameters measured in angstrom while Buckle, propeller, and opening are angle parameters and hence measured in degrees (**Table 7**). Upon closer inspection, the data suggest that these parameters are reasonably stable, with average values being near to zero. All of these displacements are either zero or extremely close to zero. Any deviation from zero causes the complex to become unstable by interfering with base pair stacking. The angle parameter opening shows consistent positive and negative values as usual. The opening toward the minor groove side is indicated by the opening's negative values. There has been no discernible specificity for the opening of base pairs in this instance. The distance parameters Shift, Slide, and Rise are also expressed in units of angstroms (Å) (**Table 8**).

Table 5. Local base pair helical parameters for the initial structure of DNA G-quadruplex.

S. No.	step	X-disp	y-disp	h-Rise	Incl.	Tip	h-Twist
1.	TG/GT	-1.34	-0.51	-3.75	-0.42	1.21	140.68
2.	GG/GG	-2.02	0.09	-0.62	-6.38	6.26	176.88
3.	GG/GG	0.27	2.01	-2.28	-35.22	81.46	171.88
4.	GG/GG	-1.76	0.72	0.89	6.4	-6.09	175.33
5.	GG/GG	-1.56	-0.03	-0.65	-14.27	87.13	178.97
6.	GG/GG	-1.89	0.3	-0.63	2.08	4.19	175.51
7.	GG/GG	-2.01	0.75	0.8	39.04	-77.91	170.25
8.	GT/TG	…..	…….	…..	……	…….	…….
9.	TG/GT	-0.71	0.57	-3.62	0.66	-0.37	128.71
10.	GT/TG	…….	…….	…….	……	…….	…….
11.	TG/GT	-0.06	-2.26	-3.84	-4.99	-2.83	114.86
12.	GG/GG	-1.28	1.02	-2.03	-79.36	-33.37	-175.56
13.	GG/GG	-1.71	1.02	1.29	7.67	-1.34	167.73
14.	GG/GG	1.41	1.03	1.29	17.43	-86.86	-177.09
15.	GG/GG	-1.87	0.4	-0.55	2.31	7.05	173.91
16.	GG/GG	-1.79	0.25	1.42	34.38	-78.51	168.53
17.	GG/GG	-2.05	0.19	0.24	-2.79	-0.33	172.39
18.	GT/TG	-0.4	1.27	3.46	2.4	-3.76	-120.81
19.	TG/GT	…….	…….	…….	…….....	…….	…….
	Ave.	-1.17	0.43	-0.54	-1.94	-6.5	102.64
	Sd.	1.01	0.93	2.11	26.93	48.04	131.06

Here, we can see that the numbers are fluctuating and are close to the B-form DNA. As a natural result of the finite backbone Chain length from one base pair to the next, any change in the angle parameters—Tilt, Roll, and Twist may be viewed as dislocations (**Table 8**). Compression on the minor groove side is indicated by the Roll parameter's positive sense. The inter-base pair displacements' local expansion with

respect to the minor groove side is defined by the Roll and Tilt parameters. The dynamic behaviour of the DNA quadruplex model and its initial conformation are explained in full by the calculations presented here. From related data, we find that the parameters do not change. This suggests that there is stability in the quadruplex. This is due to the fact that as temperature rises, atom's kinetic energy also rises, intensifying vibrations and instability that ultimately cause the DNA quadruplex to break.

Table 6. Local base pair helical parameters for the final structure(100ns).

S. No.	step	x-disp	y-disp	h-rise	incl.	tip	h-twist
1.	GG/GG	1.02	-1.75	0.27	64.95	59.96	173.38
2.	GG/GG	-1.16	-5.96	5.38	28.52	-16.53	43.52
3.	GG/GG	-2.25	-1.78	4.16	15.17	0.64	47.21
4.	GG/GG	2.04	-1.38	1.57	-7.21	28.37	80.66
5.	GT/TG	1.02	0.82	6.27	5.46	-10.39	88.19
	ave.	0.14	-2.01	3.53	21.38	12.41	86.59
	s.d.	1.77	2.46	2.54	27.65	31.67	52.39

Table 7. Local base pair parameters for the final structure(100ns).

S. No.	bp	Shear	Stretch	Stagger	Buckle	Propeller	Opening
1.	G+G	-1.56	-3.71	0.03	-3.15	-8.99	85.00
2.	G+G	4.50	2.57	-1.05	14.28	9.40	-59.29
3.	G-G	-5.02	-0.52	-1.60	4.82	-52.48	-100.78
4.	G-G	6.14	-0.67	-0.07	24.19	-18.58	-115.44
5.	G+G	1.17	1.54	-1.59	-41.89	-7.34	-167.22
6.	T+T	6.30	3.61	2.00	21.73	-22.61	46.13
	ave.	1.92	0.47	-0.38	3.33	-16.76	-51.93
	s.d.	4.57	2.65	1.37	24.42	20.72	98.11

Table 8. Local base pair step parameters for the final structure(100ns).

S. No.	Step	Shift	Slide	Rise	Tilt	Roll	Twist
1.	GG/GG	3.00	2.58	0.92	-117.10	126.86	51.68
2.	GG/GG	5.71	1.36	3.85	11.67	20.14	37.03
3.	GG/GG	1.38	-0.74	4.49	-0.51	12.03	45.73
4.	GG/GG	1.00	2.45	2.37	-35.76	-9.09	73.05
5.	GG/TG	-0.32	1.86	6.25	14.40	7.57	86.98
	ave.	2.15	1.50	3.58	-25.46	31.50	58.90
	s.d.	2.31	1.34	2.04	54.99	54.36	20.57

3.4 Temperature Dependent RMSD Analysis

The root mean square deviations (RMSD) of the MD simulated structures at 300K temperatures with respect to the original structure were calculated as a function of the 100 ns interval in order to show global convergence in the DNA model **(Figure 2).** All of the model's planes had significant deviations, according to the quadruplex's RMSD analysis at 300 K. Overall, taking into account tiny variations in helicoidal structure and torsion angles, the small RMSD suggests that the DNA quadruplex structure is significantly converged at 300 K. The convergence and stability profiles presented in **Figure 2** show that the MD structure rapidly reaches a stable equilibrium position during simulation, with the coupled Chains' modest oscillations centred on 6±0.8 Å. The RMSD plot illustrates that, for all Chains (A&B), the RMSD of the heavy atoms varies in a small range centred around 6±0.8 Å when the system is constrained. Chain

A fluctuates at 25–30 ns up to 12 Ao the four strands become stable, and the oscillation range extends from 4 to 7Å. This shows that the base pairs are perturbed due to an increase in thermal fluctuations. Finally, in the plot of RMSD, we note that the deviation, which was initially changed to 5±2 Å, remains constant for all Chains of the quadruplex until the simulation ends. This can result from the entropy's contribution and the restrictions reduction in order to reach the stable conformation. We conclude that the DNA quadruplex is sensitive to temperature; even a slight change in temperature can cause nucleic acid base pair orientation to change, making DNA an essential molecule for research work (Rebič et al., 2016).

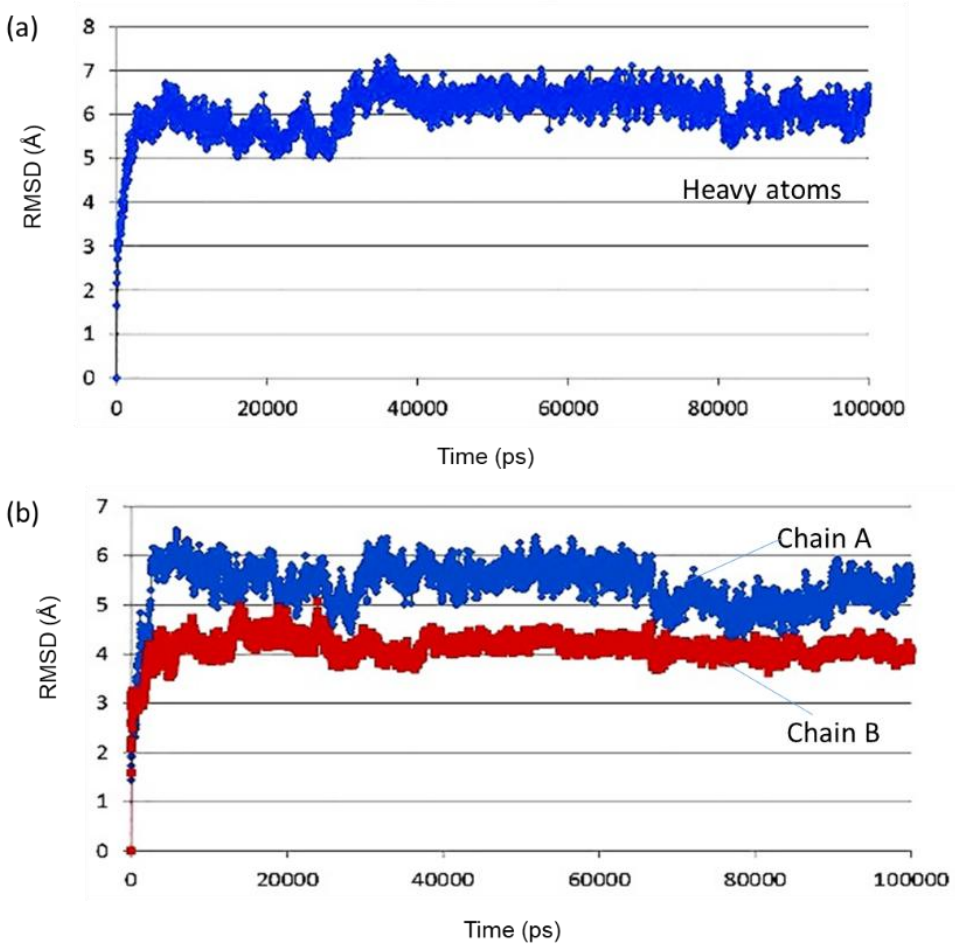

Figure 2. (a)Averaged time evolution of RMSD of the G4 structure. (b) Variation in RMSD value of Chain A and Chain B during entire MD simulation.

3.5 Temperature Dependent RMSF Analysis

The average departure of the individual residues over time from a reference position is measured by root means square fluctuation, or RMSF (**Figure 3**) shows the RMSF curve of the DNA quadruplex structure during the molecular dynamic simulation. It has been noted that no significant abrupt variations in RMSF were seen during the 100 ns of molecular dynamics simulation at 300K. Similarly, the quadruplex RMSF

investigation at 300K showed a rise in RMSF values, with chain A showing the highest RMSF. Chain B, on the other hand, remains comparatively steady (Castelli et al., 2022; Rebič et al., 2016).

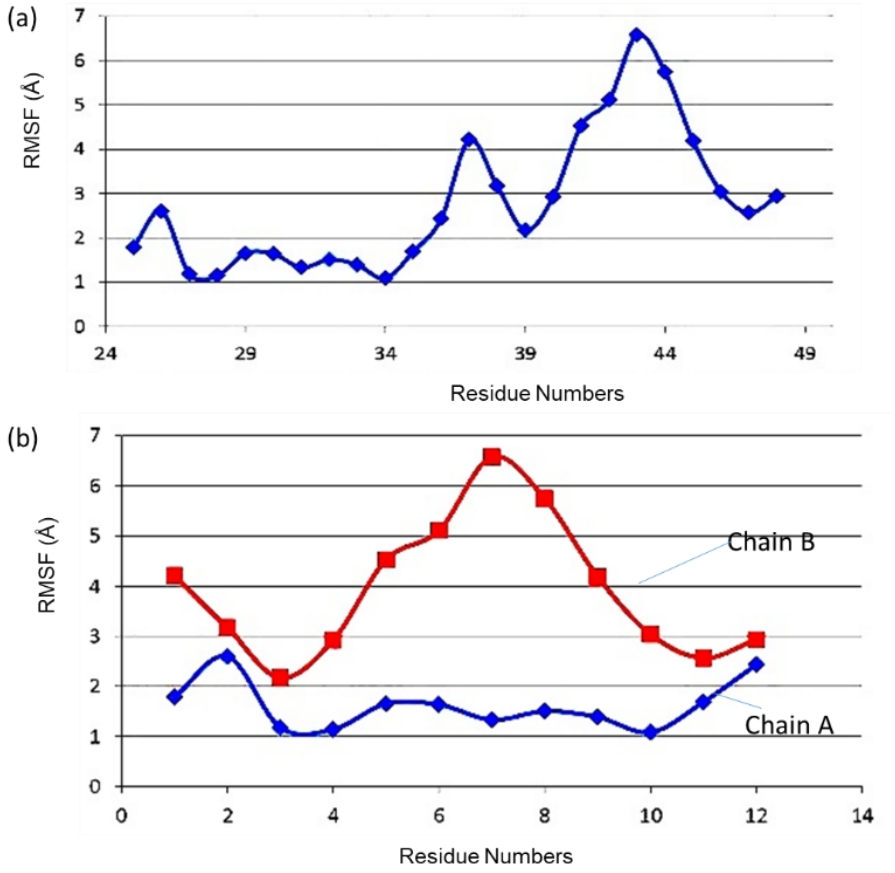

Figure 3. (a)Averaged departure of RMSF over residues of G4 structure. (b) Departure in RMSF value over residues of Chain A and Chain B of G4 structure.

3.6 Temperature Dependent Radius of Gyration (Rg)

Figure 4 shows the radius of gyration for the PDB ID 1d59 calculated after the 100 ns simulation interval for each of the chains of the DNA G-quadruplex at temperature 300K. When MD simulations were run at this temperature, From the plot, it is observed that there is a slide fluctuation in radius of gyration values of chains A & B and this variation is near about 2 Å (8.5-10.5 Å) for chain A and 1.2 Å (10-11.2 Å) for chain B. Its value for chain B shows more stability while spikes in chains A, indicate that the quadruplex structure is slightly unstable at this temperature. But at this temperature 300K there was a very abrupt oscillation in RMSF values of both the chains. In plot, the origin of the sharp jumps for Rg values is due to the movement of molecule for a shorter period of time. Hence due to such movement, the molecule alters the position for a while and again regain their position and maintained its structural rigidity and integrity.

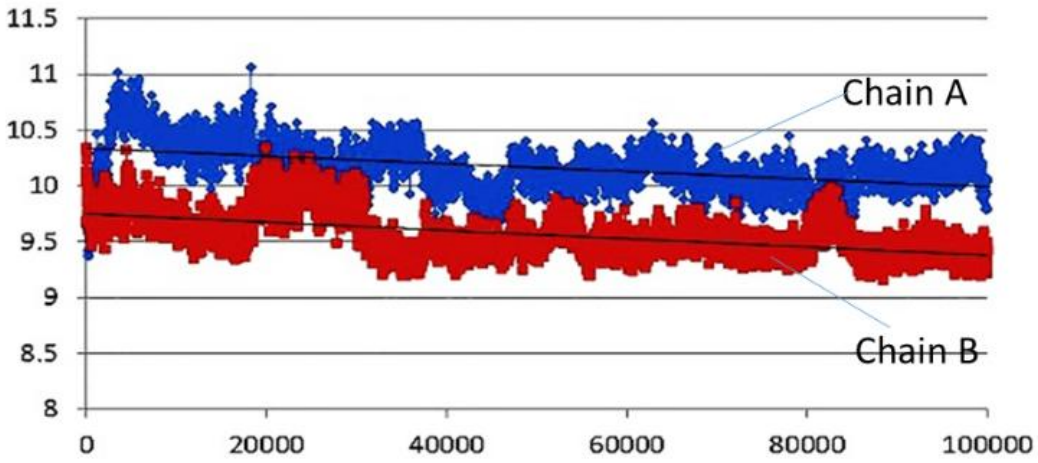

Figure 4. Fluctuation in Rg value with simulation time at 300K.

4. Conclusions

This paper explains simulation on DNA G-quadruplex built by taking the base pairs with the sequence d(GGGGTTTTGGGG) and discusses the MD simulation of the G4 quadruplex structure. A 100ns molecular dynamics run at 300K was performed and snapshots at periodic intervals of 10 ns were taken. The change in structure and conformation across the lengthy dynamical pathway was analysed. Although it appears that the quadruplex molecule's structure remains unchanged during the dynamics simulation, a closer look reveals variation in the majority of the structural and geometrical parameters, such as the helix axis parameters, RMSD, RMSF, Rg as well as the torsion angle parameters, as explained in the results and discussion section. The DNA quadruplex's conformational and torsion angle parameters provide a comprehensive picture of the molecular dynamic behaviour. The little alterations in the parameters suggest that the quadruplex exhibits a hinge point where the residue appears to be folding. According to the conformational analysis of the d($G_4T_4G_4$) DNA quadruplex at 300K, the DNA quadruplex preserved its structural integrity and conformation, over the entire 100 ns MD simulation. The force field applied here is best suited to study the proteins but less sensitive to nucleic acids. This finding was corroborated by statistical analysis of the trajectory. During MD simulations, the DNA g-quadruplex underwent both structural and conformational variations, leading to a state of equilibrium with modified values when compared to the crystal structure. In conclusion, we may say that DNA quadruplex periodic arrangements are capable for various applications. They are sensitive and can be used as inhibitor for drug-based clinical applications.

Conflict of Interest

Authors declare no potential conflict of interest.

Acknowledgments

Jwala ji Prajapati is thankful to joint CSIR-UGC for providing the JRF/NET research fellowship and also thankful to Department of physics, B.R.D.P.G. college, Deoria, U.P. for providing research facilities.

References

Batool, M., Ahmad, B., & Choi, S. (2019). A structure-based drug discovery paradigm. *International Journal of Molecular Sciences*, *20*(11), 2783. https://doi.org/10.3390/ijms20112783.

Bryan, T.M. (2020). G-quadruplexes at telomeres: friend or foe?. *Molecules*, *25*(16), 3686. https://doi.org/10.3390/molecules25163686.

Burge, S., Parkinson, G.N., Hazel, P., Todd, A.K., & Neidle, S. (2006). Quadruplex DNA: sequence, topology and structure. *Nucleic Acids Research*, *34*(19), 5402-5415.

Castelli, M., Doria, F., Freccero, M., Colombo, G., & Moroni, E. (2022). Studying the dynamics of a complex G-Quadruplex system: Insights into the comparison of MD and NMR data. *Journal of Chemical Theory and Computation*, *18*(7), 4515-4528.

Ciaco, S., Aronne, R., Fiabane, M., & Mori, M. (2024). The rise of bacterial G-quadruplexes in current antimicrobial discovery. *ACS Omega*, 9(23), 24105-25414.

Di Leva, F.S., Novellino, E., Cavalli, A., Parrinello, M., & Limongelli, V. (2014). Mechanistic insight into ligand binding to G-quadruplex DNA. *Nucleic Acids Research*, *42*(9), 5447-5455. https://doi.org/10.1093/nar/gku247.

Farag, M., & Mouawad, L. (2024). Comprehensive analysis of intramolecular G-quadruplex structures: furthering the understanding of their formalism. *Nucleic Acids Research*, *52*(7), 3522-3546.

Farag, M., Messaoudi, C., & Mouawad, L. (2023). ASC-G4, an algorithm to calculate advanced structural characteristics of G-quadruplexes. *Nucleic Acids Research*, *51*(5), 2087-2107.

Frasson, I., Pirota, V., Richter, S.N., & Doria, F. (2022). Multimeric G-quadruplexes: a review on their biological roles and targeting. *International Journal of Biological Macromolecules*, *204*, 89-102. https://doi.org/10.1016/j.ijbiomac.2022.01.197.

Haider, S., Parkinson, G.N., & Neidle, S. (2002). Crystal structure of the potassium form of an Oxytricha nova G-quadruplex. *Journal of Molecular Biology*, *320*(2), 189-200.

Huppert, J.L., & Balasubramanian, S. (2007). G-quadruplexes in promoters throughout the human genome. *Nucleic Acids Research*, *35*(2), 406-413.

Kang, C., Zhang, X., Ratliff, R., Moyzis, R., & Rich, A. (1992). Crystal structure of four-stranded Oxytricha telomeric DNA. *Nature*, *356*(6365), 126-131.

Largy, E., Mergny, J.L., Gabelica, V. (2016). Role of alkali metal ions in G-quadruplex nucleic acid structure and stability. *Metal Ions in Life Sciences*, *16*, 203-258.

Ma, Y., Iida, K., & Nagasawa, K. (2020). Topologies of G-quadruplex: biological functions and regulation by ligands. *Biochemical and Biophysical Research Communications*, *531*(1), 3-17.

Nao, S.C., Wu, K.J., Wang, W., Leung, C.H., & Ma, D.L. (2020). Recent progress and development of G-quadruplex-based luminescent assays for ochratoxin A detection. *Frontiers in Chemistry*, *8*, 767. https://doi.org/10.3389/fchem.2020.00767.

Neupane, A., Chariker, J.H., & Rouchka, E.C. (2023). Analysis of nucleotide variations in human g-quadruplex forming regions associated with disease states. *Genes*, *14*(12), 2125. https://doi.org/10.3390/genes14122125.

Rebič, M., Laaksonen, A., Šponer, J., Uličný, J., & Mocci, F. (2016). Molecular dynamics simulation study of parallel telomeric DNA quadruplexes at different ionic strengths: Evaluation of water and ion models. *The Journal of Physical Chemistry B*, *120*(30), 7380-7391.

Richel, T., Kuper, J., & Kisker, C. (2024). G-quadruplex-mediated genomic instability drives SNVs in cancer. *Nucleic Acids Research*, *52*(5), 2198-2211. https://doi.org/10.1093/nar/gkae098.

Salgado, G.F., Cazenave, C., Kerkour, A., & Mergny, J.L. (2015). G-quadruplex DNA and ligand interaction in living cells using NMR spectroscopy. *Chemical Science*, *6*(6), 3314-3320. https://doi.org/10.1039/C4SC03853C.

Spiegel, J., Adhikari, S., & Balasubramanian, S. (2020). The structure and function of DNA G-quadruplexes. *Trends in Chemistry*, *2*(2), 123-136.

Šponer, J., Islam, B., Stadlbauer, P., & Haider, S. (2020). Molecular dynamics simulations of G-quadruplexes: the basic principles and their application to folding and ligand binding. *In* Neidle, S. (ed) *Annual Reports in Medicinal Chemistry* (Vol. 54, pp. 197-241). Academic Press. https://doi.org/10.1016/bs.armc.2020.04.002.

Sun, Z.Y., Wang, X.N., Cheng, S.Q., Su, X.X., & Ou, T.M. (2019). Developing novel G-quadruplex ligands: From interaction with nucleic acids to interfering with nucleic acid–protein interaction. *Molecules*, *24*(3), 396. https://doi.org/10.3390/molecules24030396.

Zhang, R., Shu, H., Wang, Y., Tao, T., Tu, J., Wang, C., Mergny, J.L., & Sun, X. (2023). G-quadruplex structures are key modulators of somatic structural variants in cancers. *Cancer Research*, *83*(8), 1234-1248.